17th World Conference on Earthquake Engineering, 17WCEE
Sendai, Japan - September 13th to 18th 2020

EMPIRICAL EQUATIONS FOR DEFORMATION CAPACITY OF CONVENTIONAL RC SHEAR WALLS

Z. Tuna Deger[(1)], C. Basdogan[(2)]

[(1)] *Assistant Professor, Istanbul Technical University, Earthquake Engineering and Disaster Mgmt. Institute, zeynep.tuna@itu.edu.tr*
[(2)] *Ph.D. Student, Earthquake Engineering and Disaster Mgmt. Institute, basdoganc@itu.edu.tr*

Abstract

Current brittle failure criteria assume that reaching failure leads to rapid strength loss and loss of axial load capacity. However, more realistic and economical rehabilitation solutions would be achieved if even modest nonlinear deformation capacities exist for so-called brittle failure modes. To address this, comprehensive equations for nonlinear deformation capacity are needed in earthquake-prone countries where accurate performance assessment of buildings is essential. Relevant research in literature approached this topic from two aspects: one that investigates effects of wall properties on deformation capacity by conducting experimental research and another that estimates deformation capacity based on analytical studies. This study aims to combine the two approaches both by making use of the experimental research to develop practical and interpretable empirical expressions for deformation capacity of conventional RC shear walls. One novel aspect of this study is that deformation capacity is expressed in terms of curvature ductility for ductile walls, unlike available literature which typically studied deformation capacity in terms of chord rotation. Based on a detailed wall test database consisting of conventional reinforced concrete walls representing the existing building stock, statistical studies were conducted to assess nonlinear deformation capacity of shear walls as well as to develop empirical relations depending on expected wall behavior. As the database was supposed to represent conventional shear walls that are typically used in existing buildings, the following specimens were excluded: (i) walls that have openings, weakened plane joints, confinement devices (versus reinforcing steel) or diagonal bars in the web, (ii) those constructed with high-strength materials, (iii) walls with no web reinforcement, and (iv) repaired and retested walls. To understand ductility behavior of shear walls under seismic loading, specimens tested under monotonic loading and those missing experimental load-deformation relations were also not considered. Deformation capacity of each specimen was obtained based on backbone curves which were generated for cyclic base shear – top lateral displacement curves by taking the average of responses in positive and negative regions. Deformation capacity was defined as drift ratio at failure and curvature ductility for shear-controlled (typically squat) walls and flexure-controlled (relatively slender) walls, respectively. Mean drift ratio at failure was obtained as about 1% for shear-controlled walls, whereas mean curvature ductility was around 4.6 for flexure-controlled walls. Regression analyses were carried out to obtain easy-to-use and interpretable equations for deformation capacity based on wall failure modes in terms of key wall parameters. The empirical equations were derived by utilizing basic machine learning techniques, that is, the equations were first derived using "training" data and then validated using novel data that have not been used in the training process. This procedure has become popular in the scientific community as it helps to enhance generalization capability of the equations. The proposed equations are compatible with the physical behavior of shear walls and are shown to estimate deformation capacity of conventional walls reasonably close to actual (experimental) values.

Keywords: reinforced concrete shear walls; deformation capacity; curvature ductility; drift ratio; empirical equations

1. Introduction

Since reinforced concrete shear walls are expected to enhance lateral strength, stiffness, and deformation capacity against wind and earthquake loads, they have been commonly used in seismically active regions. Lateral load capacity, rigidity, and ductility levels are found to be important features to characterize behavior of shear walls. Expressions and specifications for strength and stiffness are given in current seismic codes [1, 2, 3]. However, information presented in modern seismic codes related to ductility is relatively limited. As the majority of the shear wall buildings in the existing building stock were constructed before current seismic

codes were introduced, they experienced severe damage due to their inadequate detailing and material properties [4, 5]. To reduce possibility of experiencing damages in future earthquakes, those buildings are need to be modelled close to accurate. Modeling of existing buildings with performance-based design approach requires a good definition of failure in terms of deformation capacity. This study aims to assess deformation capacity of reinforced concrete shear walls and to investigate influence of various parameters on deformation capacity using a detailed wall test database.

There are relatively limited research that focused on deformation capacity in the literature. Oh et al. [6] and Hube et al. [7] stated that longitudinal boundary reinforcement and confinement in boundary region increase wall deformation capacity by conducting experimental research. Lefas et al. [8] have showed negative influence of axial load on deformation capacity. Expressions and limit values for yield and ultimate wall rotation are given by Kazaz et al. [9] using results of a parametric study. Influence of wall parameters on deformation behavior for slender reinforced concrete shear walls were investigated by Dazio et al. [10] by conducting an experimental study, whereas a large experimental database was used by Grammatikou et al. [11] to develop empirical expressions to define wall chord rotation.

In this study, a detailed wall test database is used to derive practical expressions for deformation capacity of RC shear walls. An important aspect of this study is that drift ratio at failure and curvature ductility were used to express deformation capacity. Another important aspect is that predictive equations suggested in this study were derived using basic machine learning skills, i.e. equations were derived using training data and then tested using validation data that were not used while deriving the equations.

2. Relation Between Shear Stress – Deformation Capacity

There are several studies in literature indicating the relation between deformation capacity and level of shear strength [12, 13, 14]. For example, in the experimental study conducted by Orakcal et al. [12] shear strength and deformation capacity levels of two wall pier specimens (WP-T5-N0-S2 and WP-T5-N10-S1) with same geometry and reinforcement configuration but different axial load levels ($P/A_g f_c = 0$ and $P/A_g f_c = 0.10$ respectively) were compared. Test results showed that these specimens have failed at different levels of shear stress such that the wall that failed at higher shear stress level (WP-T5-N10-S1) was able to reach lower deformation capacity. Negative correlation between deformation capacity and shear stress level was stated also by Oesterle et al. [13] by giving cyclic load- displacement curves of two specimens (B3 and B5) with same geometry and axial load levels ($P/A_g f_c = 0$) but different reinforcement configurations. Test results showed as given in Fig. 1 that lower deformation capacity was observed for specimen B5, which has reached an ultimate shear stress at $7\sqrt{f_c}$, whereas deformation capacity was higher for specimen B3 that reached a lower shear stress level as $4\sqrt{f_c}$.

The negative correlation between shear stress and deformation capacity stated in experimental studies needs to be taken into account in analytical models. Results of several previous studies [15] have demonstrated decreasing shear strength with increasing ductility as given in Fig. 1. A similar relation is given in ASCE 41-17 [1] in Fig. 2 for columns which suggests considering shear-flexure interaction by reducing shear strength with increasing ductility with a reduction factor (k).

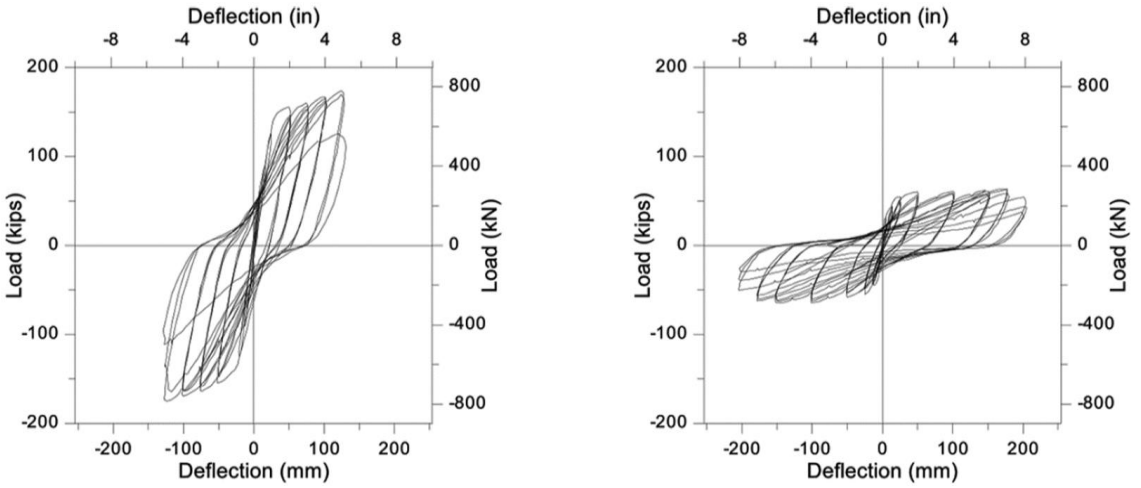

a) Specimen B5 (high shear – low ductility) , b) Specimen B3 (low shear – high ductility)

Fig. 1 – Wall cyclic load behavior shear strength versus ductility relation [13]

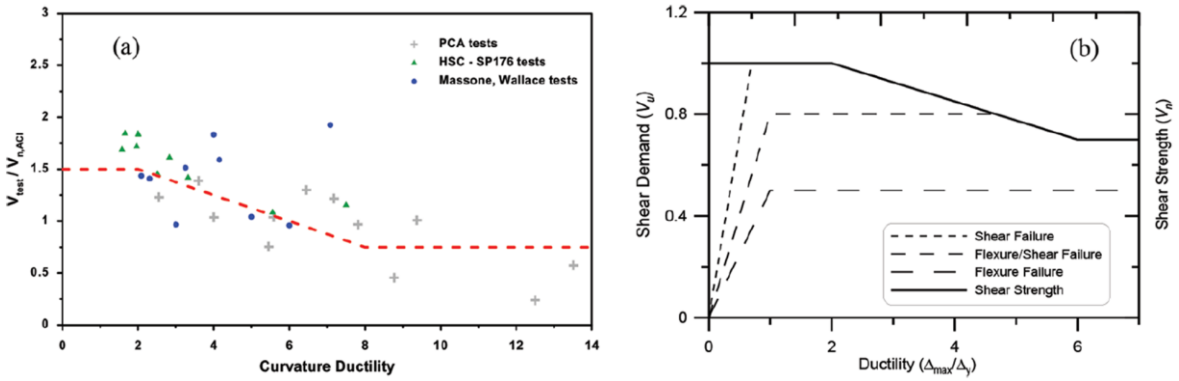

Fig. 2 – (a) Shear strength vs. curvature ductility [9]; (b) Column Shear Strength-Demand Relation [11]

Assessment of the negative correlation between ductility and shear strength, as well as nonlinear deformation capacity of walls that have different failure modes were studied. Assessing nonlinear deformation capacity of shear-controlled walls was particularly important as it would show whether even modest nonlinear deformations exist for walls that have brittle failure modes so that seismic retrofit of existing buildings would become more economical.

To achieve aforementioned goals of the study, a detailed wall test database that includes a wide range of key parameters and specific points of backbone curves of each specimen to make a comprehensive study on wall deformation capacity possible was assembled. After the wall test database was created, specimens in the database were categorized as shear-controlled walls, transition walls, and flexure-controlled walls according to their reported failure modes. In this paper, results of statistical analyses on deformation capacity were provided and empirical equations to estimate deformation capacity of shear walls with different failure modes in terms of key parameters were derived using regression analyses and basic machine learning techniques.

The majority of the modern seismic codes do not suggest an expression for deformation capacity. As an example for information related to deformation capacity, deformation limits for shear walls are given by ASCE (adopting FEMA 356 [16]) as given in Table 1. However, these limits do not provide exact values for deformation capacity of shear walls. On the other hand, Empirical equations derived in this study will enable

engineers to use only key parameters to calculate deformation capacity in terms of drift ratio and curvature ductility.

Table 1 – ASCE 41-17 acceptance criteria for deformation capacity of RC walls

Flexure-controlled walls				**Shear-controlled walls**	
$\frac{(A_s - A_s')f_y + P}{t_w l_w f_c}$	$\frac{V}{t_w l_w \sqrt{f_c}}$	**Confined Boundary**	**Chord Rotation**	$\frac{(A_s - A_s')f_y + P}{t_w l_w f_c}$	**Total Drift, %**
≤0.1	≤4	Yes	0.020	<0.05	2.0
≤0.1	≥6	Yes	0.015	>0.05	1.0
≥0.25	≤4	Yes	0.012		
≥0.25	≥6	Yes	0.010		
≤0.1	≤4	No	0.015		
≤0.1	≥6	No	0.010		
≥0.25	≤4	No	0.005		
≥0.25	≥6	No	0.004		

3. Test Database

After a comprehensive literature review, a database was assembled using 177 specimens from 41 different studies conducted worldwide. As this study focuses on assessment of deformation capacity of conventional shear walls used in existing buildings, specimens that have diagonal bars, openings or weakened plane joints, specimens which contains high-strength materials, repaired or strengthened specimens and specimens with no web reinforcement were not included in the database.

Several key parameters mentioned in the database are as follows: length (l_w), thickness (t_w), and height (h_w) of the specimens, axial load level ($P/A_g f_c$), aspect ratio (h_w/l_w) and shear span ratio (M/Vl_w), support conditions (cantilever or fixed-fixed), compressive strength of concrete (f_c), mechanical properties and ratio of reinforcement in different region and direction (for longitudinal boundary, boundary transverse vertical web and horizontal web as $f_{ybl}-\rho_{bl}$, $f_{ysh}-\rho_{sh}$, $f_{yl}-\rho_l$, and $f_{yt}-\rho_t$, respectively). The following additional information were also included in the database as they were used in classification of specimens: cross-section type (130 rectangular and 47 nonrectangular specimens), curvature type (152 single- and 25 double-curvature specimens), and failure type (50 shear-controlled, 58 flexure-controlled, and 68 shear-flexure interaction). Failure modes were determined based on their reported damages and crack patterns. Typical geometric properties of the walls with typical reinforcement configuration is given in Fig. 3, whereas the range of key walls parameters is summarized in Table 2.

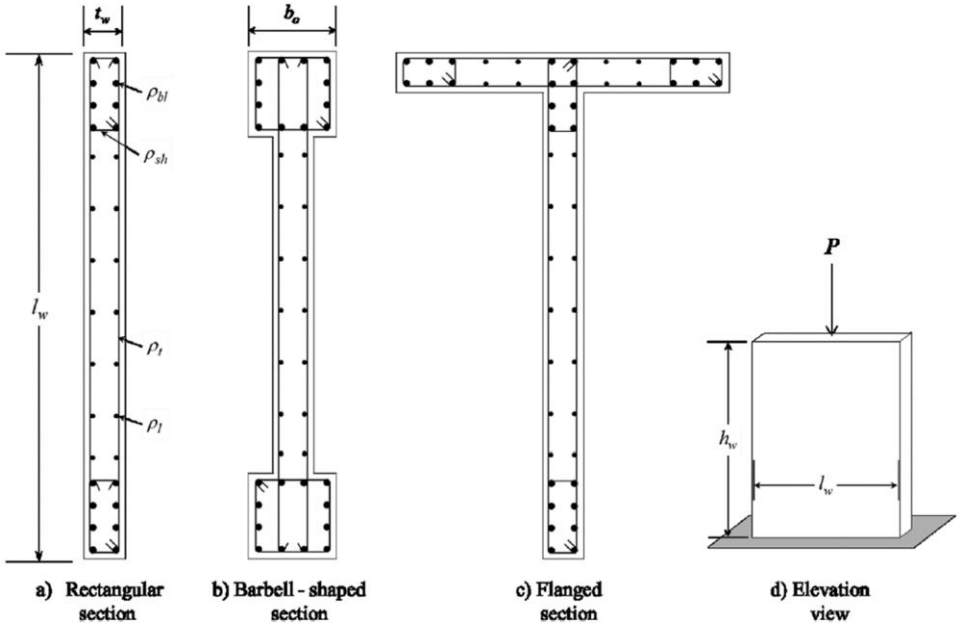

Fig. 3 – Geometrical properties reinforcement regions of reinforced concrete shear wall specimens

Table 2 – Summary of specimens in database

	Shear-controlled (50 specimens)				**Transition (69 specimens)**				**Flexure-controlled (58 specimens)**			
	Rectangular		Non-rectangular		Rectangular		Non-rectangular		Rectangular		Non-rectangular	
	Min	Max	Min	Max	Min	Max	Min	Max	Min	Max	Min	Max
h_w, cm	70	200	15	215	69	1200	48	457	120	640	225	1200
l_w, cm	58.5	300	43	191	40	305	191	239	40	265	100	163
t_w, cm	6.0	15.2	1.6	10.2	4.5	30	10.2	10.2	6	20	6	20
M/Vl_w	0.35	2	0.35	1.43	0.69	4.1	0.25	2.39	0.91	4.1	1.5	7.38
$P/A_g f_c$	0	0.3	0	0	0	0.5	0	0.13	0	0.4	0.08	0.22
f_c, MPa	15.7	37	13.8	36.6	21.6	57.5	21.2	53.6	15.4	50.2	15.4	49
f_{ysh}, MPa	366	552	382	478	372	610	440	525	289	584	342	620
ρ_{sh}, %	0	1.13	0.15	0.91	0	2.09	0.16	1.36	0	1.51	0.1	2.04
f_{ybl}, MPa	314	533	382	489	276	702	410	539	289	601	345	540
ρ_{bl}, %	0	1.79	0.34	0.85	0	1.31	0.32	1.07	0.1	1.5	0.16	0.91
f_{yt}, MPa	305	608	323	496	216	610	440	525	262	608	345	562
ρ_t, %	0.13	1.0	0.34	0.79	0.15	1.67	0.27	1.37	0.25	1.11	0.26	0.44
f_{yl}, MPa	305	608	323	527	216	601	440	545	289	584	342	562
ρ_l, %	0.13	3.29	0.34	0.71	0.15	2.91	0.21	0.82	0.24	1.55	0.24	0.42

To collect information related to deformation capacity, backbone curves were also needed. Backbone curves were created by approximating four linear lines, i.e. five points corresponding to: origin, crack point,

yielding point, maximum lateral force, and maximum lateral displacement. The backbone curves were created for both positive and negative regions and backbone coordinate values used in statistical analyses were calculated as the average of responses in positive and negative regions. A typical cyclic load-displacement response is shown in Fig. 4.

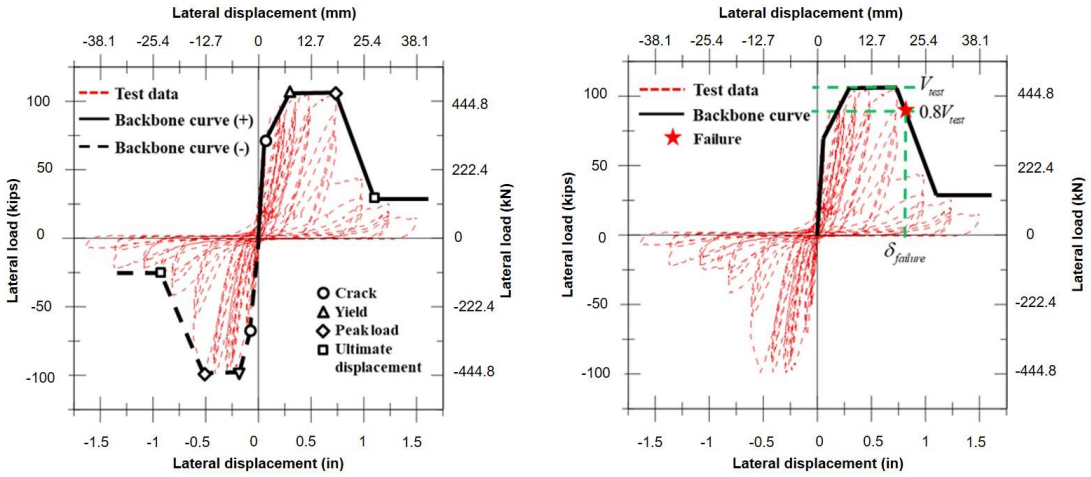

Fig. 4 – Load-deformation response of reinforced concrete specimens

4. Definition of Failure

Results of the experimental studies presented by Oesterle et al. [13] showed that a certain level of deformation can be reached without a significant loss in lateral load capacity. However, at the maximum displacement point of the backbone curve, corresponding lateral load becomes much less than the maximum lateral load level. On the other hand, in the study conducted by Park [17], displacement where the specimen lost 20% of its lateral load capacity has been used for ductility calculations. In this paper, statistical analyses on deformation capacity and ductility were conducted using the displacement that corresponds 80% of the maximum shear (V_{test}) based on the same assumption and the displacement at that level was named as failure displacement (δ_f) as shown in Fig. 4.

Deformation capacity of specimens with different failure types were investigated in terms of failure drift ratio (Δ_f) and curvature ductility ($\mu_{\phi f}$). Failure drift ratio was obtained for each specimen by dividing failure displacement to corresponding wall height ($\Delta_f = \delta_f / h_w$). Drift ratio is an important feature to characterize deformation capacity of shear walls. However, for ductile walls that span multiple levels, curvature ductility was calculated using normalized values of failure deformation. Calculation steps of curvature ductility are given for cantilever and fixed-fixed shear walls in Eq. (1) and Eq. (2), respectively.

$$\phi_y = 3\frac{\delta_y}{h_w^{\,2}},\ \phi_f = \phi_y + 2\frac{\delta_f - \delta_y}{h_w l_w},\ \text{and}\ \mu_\phi = \frac{\phi_f}{\phi_y}\ \text{(cantilever)} \tag{1}$$

$$\phi_y = 6\frac{\delta_y}{h_w^{\,2}},\ \phi_f = \phi_y + 2\frac{\delta_f - \delta_y}{h_w l_w},\ \text{and}\ \mu_\phi = \frac{\phi_f}{\phi_y}\ \text{(fixed-fixed)} \tag{2}$$

The relation between yield curvature (ϕ_y) and yield displacement (δ_y) was obtained for walls with different curvature types using elastic beam theory as given in relevant expressions (Eq. (3) and Eq. (4) for

cantilever and fixed-fixed walls, respectively), whereas ultimate curvature (ϕ_f) was derived using inelastic deformations, which has been assumed to occur over a plastic hinge length of $0.5l_w$.

$$\delta_y = \frac{Ph_w^3}{3EI} = \frac{M_y}{h_w}\frac{h_w^3}{3EI} = \frac{h_w^2}{3}\left[\frac{M_y}{EI}\right] = \frac{h_w^2}{3}\phi_y \text{ (cantilever)} \quad (3)$$

$$\delta_y = \frac{Ph_w^3}{12EI} = \frac{2M_y}{h_w}\frac{h_w^3}{12EI} = \frac{h_w^2}{6}\left[\frac{M_y}{EI}\right] = \frac{h_w^2}{6}\phi_y \text{ (fixed-fixed)} \quad (4)$$

Experimental deformation capacity values for specimens with different failure types are summarized in Table 3 in terms of drift ratio and curvature ductility by indicating their minimum, maximum, mean, and standard deviation values. Mean curvature ductility was estimated as 3.16, 3.98, and 4.58 for shear-controlled, transition, and flexure-controlled walls, respectively. Mean values demonstrated an increasing trend from shear-controlled walls to flexure-controlled walls, as expected. Another aspect of the values summarized in Table 3 was that the mean curvature ductility of rectangular walls with constant thickness was approximately 40% less than that of the nonrectangular walls with barbells or flanges. Main reason of this difference was that the majority of rectangular walls in the database were missing a confined boundary region, indicating that transverse and longitudinal reinforcement ratios at boundary regions were much higher for nonrectangular walls.

Table 3 – Experimental deformation capacities for different failure types

		Shear-controlled (50 specimens)		**Transition (69 specimens)**		**Flexure-controlled (58 specimens)**	
		[Min Max]	**($\mu \pm \sigma$)**	**[Min Max]**	**($\mu \pm \sigma$)**	**[Min Max]**	**($\mu \pm \sigma$)**
(Δ_f,%)	ALL	[0.21 2.43]	1.01 ± 0.52	[0.71 5.46]	2.20 ± 0.95	[0.42 3.96]	1.84 ± 0.87
	R*	[0.45 2.43]	1.13 ± 0.49	[0.71 4.70]	2.00 ± 0.86	[0.42 3.96]	1.70 ± 0.87
	NR*	[0.21 2.13]	0.85 ± 0.53	[1.68 5.46]	2.94 ± 0.91	[1.40 3.39]	2.49 ± 0.60
($\mu_{\phi f}$)	ALL	[1.27 15.03]	3.16 ± 2.89	[1.62 11.17]	3.98 ± 1.95	[1.76 24.08]	4.58 ± 3.27
	R	[1.27 4.15]	1.92 ± 0.63	[1.62 8.29]	3.55 ± 1.45	[1.76 13.36]	4.10 ± 1.98
	NR	[1.57 15.03]	4.74 ± 3.79	[2.05 11.17]	5.54 ± 2.68	[2.79 24.08]	6.89 ± 6.32

*Wall cross sections: R is rectangular, NR is nonrectangular

Since shear-controlled walls are not expected to have inelastic curvature, deformation capacity of shear-controlled walls was investigated in terms of drift ratio. Normalized force-deformation responses are given in Fig. 5. Vertical axes show lateral load that normalized by shear strength obtained by ACI 318-14 [2], whereas horizontal axes show total drift ratio for shear-controlled walls and normalized curvature for transition and flexure-controlled walls, respectively.

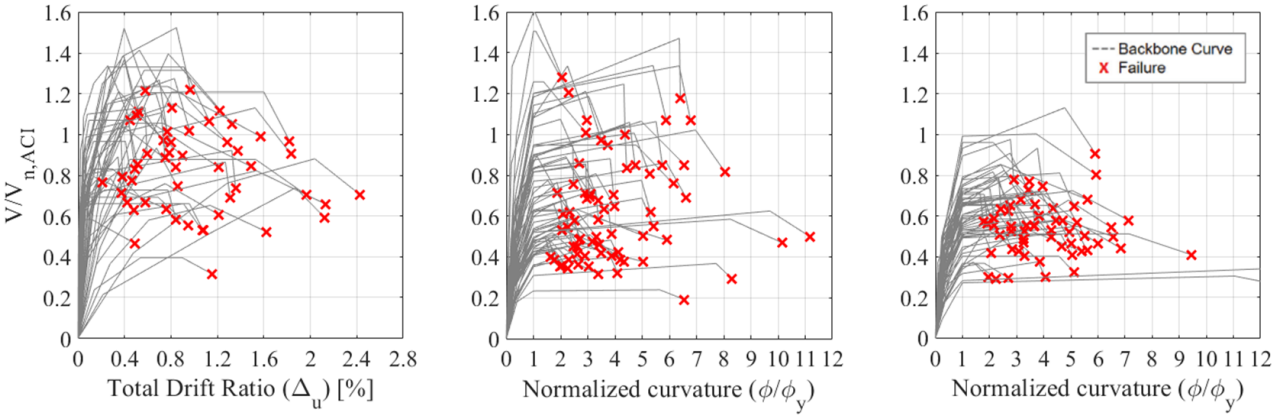

Fig. 5 – Normalized force-deformation responses

5. Statistical Analyses

Statistical studies in this paper have focused on deriving an equation that includes key wall parameters to estimate deformation capacity in terms of drift ratio for shear-controlled walls and in terms of curvature ductility for transition and flexure-controlled walls. There were three main concerns while deriving empirical expression using multi-linear regression analyses: (I) using minimum number of key parameters to make proposed equations easy-to-use, (ii) validation of equation both statically and physically, and (iii) obtaining high accuracy. To enable an effective validation of derived expressions, specimens in the database were divided randomly into two groups as "training" and "validation" data, where the training data was used for fitting and validation data was used for testing the derived equation with novel data. Training data and validation data were never mixed. Number of specimens in different bins is summarized in Table 4 in terms of failure type, cross-section type, and dataset type of the specimens.

Table 4 – Number of specimens in different bins

Wall Type		**Number of specimens**		
		Training data	**Validation data**	**Total**
Shear-controlled	**Rectangular**	14	14	28
	Non-rectangular	12	10	22
Transition	**Rectangular**	28	26	54
	Non-rectangular	9	6	15
Flexure-controlled	**Rectangular**	24	24	48
	Non-rectangular	6	4	10

Proposed equations derived after regression analyses using training data were tabulated in Table 5, which indicates that shear span ratio (M/Vl_w) or aspect ratio (h_w/l_w) increase the deformation capacity for all failure types. It is also stated that axial load ratio ($P/A_g f_c$) decreases deformation capacity as indicated in studies conducted by Lefas et al. [8] and Farvashany et al. [18]. Effect of longitudinal boundary reinforcement ratio (ρ_{bl}) on curvature ductility of transition and flexure-controlled walls was positive as given in derived equations because yielding of longitudinal boundary reinforcement may suppress brittle failure, which results inelastic deformations. The difference in curvature ductility between rectangular and nonrectangular shear walls has been considered by implementing the ratio of boundary element thickness to web thickness (b_0/t_w) into equations, which is equal to 1 for rectangular walls and greater than 1 for

nonrectangular walls. On the other hand, as shown in the proposed equation for drift ratio of shear-controlled walls, boundary confinement ratio (ρ_{sh}) has a positive impact on deformation capacity as stated in literature (e.g. study conducted by Tasnimi [19]).

Table 5 – Summary of proposed equations for deformation capacity

Wall failure type	Equation
Shear-controlled	$\Delta_{f,proposed} = -2\frac{P}{A_g f_c} + 0.55(h_w/l_w) + 0.44(1+\rho_{sh})$
Transition	$\mu_{\phi f,proposed} = -6.4\frac{P}{A_g f_c} + 2.0(M/Vl_w) + 0.2(1+\rho_{bl})\left(\frac{b_0}{t_w}\right)$
Flexure-controlled	$\mu_{\phi f,proposed} = -6.8\frac{P}{A_g f_c} + 2.5(M/Vl_w) + 0.16(1+\rho_{bl})\left(\frac{b_0}{t_w}\right)$

Validation of proposed equations indicates the reliability of equations using mean and standard deviation values of experimental-to-estimated ratios. Mean values and standard deviations ($\mu \pm \sigma$) for experimental-to-estimated ratio based on proposed equations are summarized in Table 6 as well as the experimental and estimated values for deformation capacity. As shown in Table 6, ratio used to validate reliability was close to 1 for each failure and cross-section types, which implies that the proposed equations can estimate deformation capacity reasonably close to accurate.

Table 6 – Validation of proposed equation model

	Shear-controlled walls (Δ_f,%)			**Transition walls ($\mu_{\phi f}$)**			**Flexure-controleld walls ($\mu_{\phi f}$)**		
	All	**R***	**NR***	**All**	**R***	**NR***	**All**	**R***	**NR***
Experimental	1.05±0.5	1.14±0.4	0.92±0.6	3.71±1.9	3.18±1.0	6.01±3.1	3.99±1.4	3.86±1.5	4.78±0.7
Estimated	1.07±0.3	1.19±0.3	0.91±0.3	4.07±1.6	3.74±1.4	5.51±1.6	4.47±1.6	4.29±1.3	5.53±2.9
Exp./Est.	0.99±0.4	0.99±0.3	1.02±0.6	1.01±0.6	0.98±0.6	1.11±0.5	0.97±0.4	0.95±0.4	1.05±0.5

*Wall cross sections: R is rectangular, NR is nonrectangular

6. Summary and Conclusions

Deformation capacity is one of the important features that characterizes nonlinear behavior of RC shear walls. Therefore, estimation of deformation capacity close to actual values is necessary to achieve accurate analytical models. Deformation capacity of conventional reinforced concrete shear walls were assessed in this paper using a detailed wall test database that includes wall parameters and test results of 177 reinforced concrete shear wall specimens. Specimens in the database were divided into three groups according to their failure modes as shear-controlled, transition, and flexure-controlled walls and number of specimens used in statistical analyses was 50, 69, and 58 for these groups respectively.

Conclusions of the study are summarized as follows:

- Wall deformation capacity depends on the shear stress level.
- Shear-controlled walls that show “brittle” failure have some nonlinear deformation capacity.

- Statistical studies for deformation capacity of shear walls were carried out in terms of total drift ratio at failure (Δ_f), and curvature ductility ($\mu_{\phi f}$).
- Drift ratio at failure is used to assess deformation capacity of shear-controlled walls and mean value is calculated as 1%, whereas the deformation capacity of transition and flexure-controlled walls was assessed using curvature ductility. The average of curvature ductility was about 4 and 4.6 for transition and flexure-controlled walls respectively.
- Key wall parameters were used in statistical studies and regression analyses to derive empirical equations for deformation capacity in terms of drift ratio of shear-controlled walls and curvature ductility of transition and flexure-controlled walls. The derived equations are found to be easy-to-use, consistent with the physical behavior, and are able to predict actual values accuracy.

7. Acknowledgements

The project has been supported by funds from the Scientific and Technological Research Council of Turkey (TUBITAK) under Project No. 114M264. Opinions, findings, and conclusions in this paper are those of the author and do not necessarily represent those of the funding agency. The author would like to acknowledge professors Polat Gulkan at Middle East Technical University and Kutay Orakcal at Bogazici University for their valuable contributions to this study, as well as Caglar Inceoglu (MS graduate at Istanbul Technical University) for his contribution.

8. References

[1] ASCE/SEI 41-17 (2017): Seismic evaluation and retrofit of existing buildings. *American Society of Civil Engineers*, Reston, VA, USA.

[2] ACI Committee 318 (2014): Building code requirements for structural concrete (ACI 318-14) and commentary (ACI 318R-14). *American Concrete Institute*, Farmington Hills, MI, USA.

[3] EuroCode 8 (2005): Design of structures for earthquake resistance – part 3: Assessment and retrofitting of buildings (BS EN 1998-3). *European Committee for Standardization*, Brussels, Belgium.

[4] Wallace JW, Massone LM, Bonelli P, Dragovich J, Lagos R, Lüders C, Moehle J (2012): Damage and implications for seismic design of RC structural wall buildings. *Earthquake Spectra*, **28** (S1), S281-S299.

[5] FEMA 454 (2006): Design for earthquakes: A manual for architects. *Federal Emergency Management Agency*, Washington, DC, USA.

[6] Oh YH, Han SW, Lee LH (2002): Effect of the boundary element details on the seismic deformation capacity of structural walls. *Earthquake Engineering & Structural Dynamics*, **31** (8), 1583-1602.

[7] Hube MA, Marihuen A, de la Llera JC, Stojadinovic B (2014): Seismic behavior of slender reinforced concrete walls. *Engineering Structures*, **80**, 377-388.

[8] Lefas ID, Kotsovos MD, Ambraseys NN (1990): Behavior of reinforced concrete structural walls: Strength, deformation characteristics, and failure mechanism. *ACI Structural Journal*, **87** (1), 23-31.

[9] Kazaz I, Gulkan P, Yakut A (2012): Deformation limits for structural walls with confined boundaries. *Earthquake Spectra*, **28** (3), 1019-1046.

[10] Dazio A, Beyer K, Machmann H (2009): Quasi-static cyclic tests and plastic hinge analysis of RC structural walls. *Engineering Structure*, **31** (7), 1556-1571.

[11] Grammatikou S, Biskinis D, Fardis MN (2015): Strength, deformation capacity and failure modes of RC walls under cyclic loading. *Bulletin of Earthquake Engineering*, **13** (11), 3277-3300.

[12] Orakcal K, Massone LM, Wallace JW (2009): Shear strength of lightly reinforced wall piers and spandrels. *ACI Structural Journal*, **106** (4), 455-465.

[13] Oesterle RG, Fiorato AE, Corley WG (1981): Reinforcement details for earthquake-resistant structural walls. *Research and Development Bulletin*, Portland Cement Association, Skokie, IL, USA.

[14] Thomsen JH, Wallace JW (2014): Displacement-based design of slender reinforced concrete structural walls – experimental verification. *ASCE Journal of Structural Engineering*, **130** (4), 618-630.

[15] Deger ZT (2012): Seismic performance, modeling, and failure assessment of reinforced concrete shear wall buildings. *PhD Dissertation*, University of California, Los Angeles, CA, USA.

[16] FEMA 356 (2000): Prestandard and commentary for the seismic rehabilitation of buildings. *Federal Emergency Management Agency*, Washington, DC, USA.

[17] Park R (1988): Evaluation of ductility of structures and structural assemblages from laboratory testing. *Bulletin of the New Zealand National Society for Earthquake Engineering*, **22** (3), 155-166.

[18] Farvashany FV, Foster SJ, Rangan BV (2008): Strength and deformations of high-strength concrete shear walls. *ACI Structural Journal*, **105** (1), 21-29.

[19] Tasnimi AA (2000): Strength and deformation of mid-rise shear walls under load reversal. *Engineering Structures*, **22** (4), 311-322.

